DINAME 2019 - Proceedings of the XVIII International Symposium on Dynamic Problems of Mechanics,
M.A. Savi, T.G. Ritto and W.M. Bessa (Editors), ABCM, Buzios, RJ, Brazil, March 10th to 15th, 2019

Wave attenuation in a metamaterial beam assembly with uncertainties

Adriano T. Fabro[1], **Rubens Sampaio**[2], **and Eduardo Souza de Cursi**[3]

[1] Department of Mechanical Engineering, University of Brasilia, Brasilia-DF, 70910-900, Brazil

[2] Department of Mechanical Engineering, PUC-Rio, Rio de Janeiro-RJ, 22451-900, Brazil

[3] Normandie Univ., INSA de Rouen-Normandie, LMN, BP. 8, 76801 St.-Etienne du Rouvray Cedex, France

Abstract: Metamaterials, or locally resonant metamaterials, are a class of structures that have been used to control and to manipulate acoustic and elastic waves with applications in vibration attenuation. A great amount of research has been done on acoustic and structural metamaterials but very few attention has been given to the effects of coupling conditions on structural assemblies, even though this is typical case on mechanical engineering applications. In this work, the wave attenuation in a metamaterial beam assembly is investigated considering uncertain connections. A beam, with attached resonators, undergoing longitudinal and flexural vibration is connected to homogeneous beams at each end. It is assumed a large enough number of identical resonators such that effective longitudinal and flexural wavenumbers are derived. Wave modes are assumed unchanged by the attachments and analytical expressions can be derived. A point connection is considered with an assembly angle such that wave mode conversion, between flexural and longitudinal waves, can happen. The reflection and transmission properties of the assemble are then calculated and it is shown that the angle of the assembly has a significant effect on the band gap performance. The uncertainty analysis focus on the variability of the connection angles and ensemble statistics are investigated.

Keywords: Metamaterial, band gap, structural assembly, stochastic modelling

INTRODUCTION

Metamaterials, or locally resonant metamaterials, are a class of structures that have been used to control and to manipulate acoustic and elastic waves (Hussein et al., 2014) with applications in vibration attenuation (Huang and Sun, 2009). Although periodicity of the resonators positioning is not required, it is used for a cell-based description of the wave propagation. In metamaterials, the attenuation effect is created due to inclusions or attachments that work as internal resonators (Liu et al., 2000) and are able to create band gaps at sub-wavelength frequencies, unlike the phononic crystals, which rely on spatial periodicity and the Bragg scattering effect (Hussein et al., 2014).

The use of a resonator for vibration control is very common in engineering applications (Den Hartog, 1985) but its efficacy is restricted to a very narrow frequency band. Some development has been proposed to widen the frequency band of actuation using adaptive or non-linear mechanisms (Brennan, 2006). The advantage of the concept introduced by locally resonant materials is that it is possible to widen the frequency band of attenuation by simply adding several resonators while keeping the same mass ratio (Sugino et al., 2017). Note that the established concepts from smart structures can also be applied to metastructures (Fan et al., 2016), improving even further its vibration attenuation Note that a single resonator attached to a host structure can also be described in terms of reflection and transmission coefficients, the concepts of negative mass and the negative group velocity, which occur at the band gap, can be interpreted by the dynamic stiffness concept and in the context periodic structures (Mace, 2014). A great amount of research has been done on acoustic and structural metamaterials (Hussein et al., 2014) but very few attention has been given to the effects of coupling conditions on structural assemblies, even though this is typical case on mechanical engineering applications.

The dynamics of joints has been investigated for many decades and several approaches have been proposed in terms of energy flow (Beshara and Keane, 1997), vibrational modes (Arruda and Santos, 1993) and wave reflection and transmission coefficients (Muggleton et al., 2007; Zhang et al., 2010). The modelling of joints in mechanical assemblies can be very challenging and usually requires the inclusion of some level of uncertainty (Ibrahim and Pettit, 2005). Typically, the mechanical properties of the joints are considered uncertain (Dohnal et al., 2009) and are handled by a parametric approach in which case a stochastic model of the parameters is used or a non-parametric approach in which case the mechanical model itself is considered to be random (Fabro and Mencik, 2018).

In this work, the wave attenuation from a metamaterial beam assembly is investigated considering parametric uncertainties. A metamaterial beam undergoing longitudinal and flexural vibration is considered and it is connected to a simple bare beam at each end. A point connection is considered with a angle such that wave mode conversion between flexural and longitudinal waves can happen. The scattering properties of the assemble can then be calculated and it is shown that the angle of the assembly has a significant effect on the band gap performance. The uncertainty analysis focus on the variability of the connection angles and ensemble statistics are investigated. Two cases are considered, one which only

one connection angle is uncertain and other which both angles are uncertain. For each case, two probabilistic models are assumed and it is shown that the choice stochastic model increases the variability of the results. It is shown that introducing connection angles between the metamaterial and the host structure can significantly increases the attenuation performance due to the wave mode conversion at the joints. Moreover, the choice of sets of random variable played a much more important role in the results than the probabilistic models for the random variables.

Wave model

The governing equation of motion of a general one-dimensional undamped system of distributed parameter can be given by

$$L(x)w(x,t) + \mu\ddot{w}(x,t) = p(x,t), \tag{1}$$

where $L(x)$ is a linear homogeneous self-adjoint stiffness differential operator of order $2q$, where $q \geq 1$ is an integer defining the order of the system, μ is the mass density per unity length, $p(x,t)$ is the force per unity length and $w(x,t)$ is the displacement. For rods undergoing longitudinal vibration $L(x) = -d/dx[EA(x)d/dx]$, where $EA(x)$ is the longitudinal stiffness, and for beams undergoing flexural vibration, $L(x) = d^2/dx^2\left[EI(x)d^2/dx^2\right]$, where $EI(x)$ is the flexural stiffness. Assuming harmonic motion such that $w(x,t) = e^{i(\omega t - kx)}$, homogeneous properties and free vibrations, where ω is the angular frequency and k is the wavenumber, then it is possible to define the dispersion relation $L(-ik) - \mu\omega^2 = 0$. Using the stiffness operators for rods and beams leads to $k_l = (\rho/E)^{1/2}\sqrt{\omega}$ and $k_b = (\rho A/EI)^{1/4}\omega^{1/2}$, which are the longitudinal and flexural wavenumbers, respectively. The displacement field in the rod $u(x,t)$ and in the beam $w(x,t)$ is then given by

$$u(x,t) = \left(a_l^+ e^{-ik_b x} + a_l^- e^{ik_b x}\right)e^{i\omega t}, \quad w(x,t) = \left(a_b^+ e^{-ik_b x} + a_{bN}^+ e^{-k_b x} + a^- e^{ik_b x} + a_{bN}^- e^{k_b x}\right)e^{i\omega t}, \tag{2}$$

where $a_l^\pm$, $a_b^\pm$ and $a_{bN}^\pm$ are the wave amplitudes of the positive and negative going propagating and non-propagating longitudinal and flexural waves, respectively. A linear transformation from the wave domain to the physical domain can be given for a generalized displacement and generalized force, respectively, by

$$\mathbf{q} = \Phi_q^+\mathbf{a}^+ + \Phi_q^-\mathbf{a}^-, \quad \mathbf{f} = \Phi_f^+\mathbf{a}^+ + \Phi_f^-\mathbf{a}^-, \tag{3}$$

where $\Phi_q^\pm$ and $\Phi_f^\pm$ are, respectively, displacement and internal forces matrices. For a waveguide undergoing both longitudinal and flexural waves, then $\mathbf{q} = [u \quad w \quad \theta]^T$ and $\mathbf{f} = [P \quad V \quad M]^T$, where $\theta = dw/dx$, P is the rod axial force, V is the beam shear force and M is the bending moment, and the wave amplitude vectors are given by $\mathbf{a}^\pm = \left[a_l^\pm \quad a_b^\pm \quad a_{bN}^\pm\right]^T$.

The equation of motion of a continuous system with S periodically attached resonators can be given in the general form by (Sugino et al., 2017)

$$L(x)w(x,t) + \mu\ddot{w}(x,t) - \sum_{p=1}^{S} k_p u_p(t)\delta(x - x_p) = p(x,t), \tag{4}$$

and one additional equation for each resonator $m_p\ddot{u}_p(t) + k_p u_p(t) + m_p\ddot{w}(x_p,t) = 0$, where $u_p(t)$ is the displacement of each resonator attached at x_p, with mass m_p and stiffness k_p and $\delta(x)$ is the Dirac delta function. This expression was originally proposed for a modal analysis in metastructures and allows the derivation of closed form expression for the band gap frequency edges. In this work, it will be used for finding the dispersion equation. Also, assuming that the wave modes are unchanged due to the resonators attachments, it provides a analytical framework for calculating reflection and transmission coefficients. Note that it is similar to Eq. 1 and thus a similar procedure can be applied for finding the dispersion equation. Assuming identical resonators and a large enough number of attachments, it can be shown that

$$L(-ik) - \mu\omega^2\left(1 + \varepsilon\frac{1}{1-\Omega_r^2}\right) = 0, \tag{5}$$

where $\Omega_r = \omega/\omega_r$ and $\omega_r^2 = k_p/m_p$ and $\varepsilon = m_p/\mu\Delta l$ is the mass ratio for resonators spaced by Δl. Derivation details are shown in the Appendix. The suitable stiffness operators can be applied to find the effective wavenumbers for longitudinal and flexural waves

$$k_{rl} = \sqrt{\frac{\rho}{E}\left(1 + \varepsilon\frac{1}{1-\Omega_r^2}\right)}\omega, \quad k_{rb} = \sqrt[4]{\frac{\rho A}{EI}\left(1 + \varepsilon\frac{1}{1-\Omega_r^2}\right)}\sqrt{\omega}. \tag{6}$$

This result is equivalent to (Gao et al., 2011) for a continuous neutralizer attached to the beam, in which the mass ratio is given in terms of wave length. Assuming that the attached resonators do not change the wave types, these wavenumbers

can then be used to describe the displacement field as given by Eq. 2, and the matrices $\Phi_q^{\pm}$, $\Phi_f^{\pm}$ are the same as for the simple beam.

Metamaterial assembly

A metamaterial beam undergoing longitudinal and flexural waves is connected to two other homogeneous beam, one at each end, as shown in Fig. 1. At the left end, the connection angle is α_1, $\mathbf{b}_1^{\pm}$ are the amplitude of the incoming and outgoing waves. At the right end, the connection angle is α_2, $\mathbf{a}_1^{\pm}$ are the amplitude of the outgoing and incoming waves. A scattering matrix can be defined relating the incoming and outgoing waves of the assembly by (Harland et al., 2001; Fabro et al., 2015)

$$\begin{bmatrix} \mathbf{a}_2^+ \\ \mathbf{b}_1^- \end{bmatrix} = \begin{bmatrix} \mathbf{r}^+ & \mathbf{t}^+ \\ \mathbf{t}^- & \mathbf{r}^- \end{bmatrix} \begin{bmatrix} \mathbf{a}_2^- \\ \mathbf{b}_1^+ \end{bmatrix}, \tag{7}$$

where $\mathbf{r}^{\pm}$ are reflection matrices and $\mathbf{t}^{\pm}$ are transmission matrices. They can be obtained from the equilibrium and continuity conditions at the beams connections and the wave propagation along the metamaterial beam. The full derivation is presented in the Appendix. Assuming $\mathbf{a}_2^- = \mathbf{0}$, i.e., a incident wave on the left end only, then the scattering simplifies to $\mathbf{a}_2^+ = \mathbf{t}^+\mathbf{b}_1^+$ and $\mathbf{b}_1^- = \mathbf{r}^-\mathbf{b}_1^+$. Therefore, the transmission coefficient $\mathbf{t}^+$ can be used as to access the vibration attenuation of the metamaterial beam in the assembly.

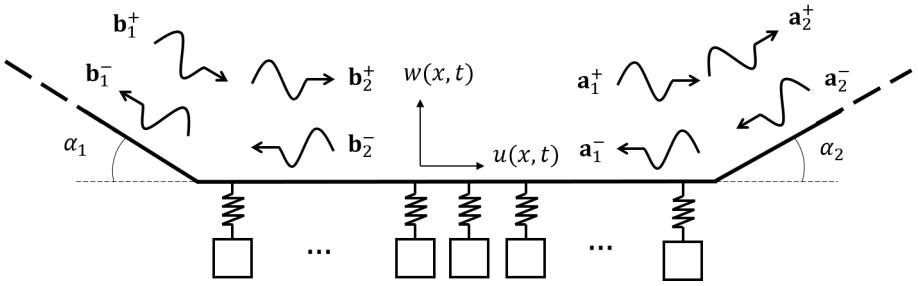

Figure 1: Metamaterial beam assembly with one semi-infinite homogeneous beam at each end undergoing longitudinal and flexural vibration.

In this case, the reflection and transmission matrices are size 3×3 and relate the longitudinal, propagating flexural and non-propagating flexural (near field) wave amplitudes at the both sides of the assembly. For $\alpha_1 = \alpha_2 = 0$, i.e., a straight assembly, no wave mode conversion is expected and these matrices are diagonal. However, for $\alpha_1 \neq 0$ and $\alpha_2 \neq 0$, they are full matrices and wave mode conversion plays a role on the metamaterial vibration attenuation performance. Moreover, asymmetries in the assembly can be given by differences in the connection angle, i.e. $\alpha_1 \neq \alpha_2$, and also play a role on the reflection coefficients $\mathbf{r}^{\pm}$, while $\mathbf{t}^+ = \mathbf{t}^-$ due to reciprocity.

PROBABILISTIC MODELLING

Two cases are considered in the analysis. In the first, it defined that the first connection angle α_1 is fixed while $\alpha_2 = \alpha_1 + \theta$, where θ is a sample of the random variable Θ. In the second case, it is considered that both connection angles α_1 and α_2 can be modelled by the random variables $\mathtt{A}_1$ and $\mathtt{A}_2$, respectively. For each analysis case 2 probabilistic models are defined. The probability distribution of the random variables have to take in to account physical constrains of the problem. Typically, manufacturing processes can only guarantee minimum θ_1 and maximum θ_2 values from the tolerances in the assembly process. It is also reasonable to assume that the angles in both connections are not correlated. Given the lack of any additional information, it is reasonable to assumed two possible probability density functions (PDF). First, the uniform PDF, i.e.

$$f^{(1)}_{\Theta,\mathtt{A}_1,\mathtt{A}_2}(x) = \frac{1}{\theta_2 - \theta_1}, \quad \theta_1 \leq x \leq \theta_2, \tag{8}$$

where θ_1 and θ_2 are the lower and the upper limits of the random variable Θ. A second model is the truncated Gaussian PDF, which is defined from a parent Gaussian distribution with mean value μ and standard deviation σ as

$$f^{(2)}_{\Theta,\mathtt{A}_1,\mathtt{A}_2}(x) = \frac{\phi\left(\frac{x-\mu}{\sigma}\right)}{\sigma\left[\Phi\left(\frac{\theta_1-\mu}{\sigma}\right) - \Phi\left(\frac{\theta_2-\mu}{\sigma}\right)\right]}, \quad \theta_1 \leq x \leq \theta_2, \tag{9}$$

where $\phi(x)$ is the normal standard PDF and Φ is the normal standard cumulative distribution function. Note that the mean and standard deviation of this truncated distribution are not μ and σ, respectively. They are altered as a effect of the truncation.

Convergence of the stochastic solution

The mean-square converge with respect to the independent realizations of the stochastic solution is a function of the number of Monte Carlo samples n_S and can be studied as (Rubinstein and Kroese, 2007)

$$conv(n_S) = \frac{1}{n_S}\sum_{j=1}^{n_S}\int_{\mathtt{B}} \left|\mathbf{t}^{+}\right| df \tag{10}$$

where $\mathtt{B}$ if the frequency bad under analysis and $\mathbf{t}^{+}$ is the frequency dependent transmission coefficient under analysis.

NUMERICAL RESULTS

In this section, numerical results are presented considering the metamaterial beam assembly. All of the beams with and without resonators are composed of polyamide, whose mechanical properties are described in (Fabro et al., 2016). The metamaterial beam is 20 cm long and the resonators have a flexural natural frequency at 900 Hz and longitudinal natural frequency at 1300 Hz. Figure 2 presents the real and imaginary part of the longitudinal and flexural wavenumber for the bare beam and the absolute value of the transmission coefficient, considering $\alpha_1 = \alpha_2 = 0$, i.e., a straight assembly. For a lossless waveguide, the wavenumber can be real, leading to a propagating wave, imaginary, giving a decaying or evanescent wave, or complex, which has both behaviours, i.e. propagating and decaying. The imaginary part of the dispersion curve (negative values) shows the frequency band in which there is vibration attenuation for each wave mode, i.e. the band gap for longitudinal and flexural waves. Note that the wave types do not interact because the axial and flexural vibration are considered uncoupled at the metamaterial beam. This is also noticed in the absolute value of the transmission coefficient, which shows a very low transmission at the band gap frequencies for each individual wave mode. Additionally, from the dispersion curve it can be seen that the group velocity $c_g = \partial\omega/\partial k$, that gives the velocity of energy transport, is zero at the resonator frequency and it is negative at the band gap.

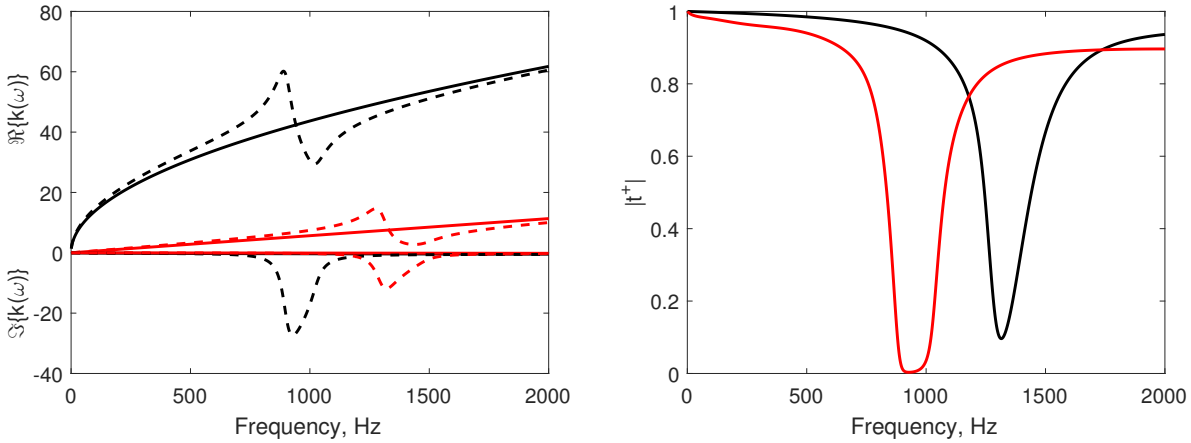

Figure 2: (a) Real and imaginary parts of the longitudinal (red) and flexural (black) wavenumbers for the bare beam (solid line) and metamaterial beam (dashed line) and (b) absolute value of the transmission coefficient considering $\alpha_1 = \alpha_2 = 0$.

Figure 3 shows the longitudinal and flexural transmission coefficient of the assembly for several values of α_1, from 0 to $\pi/2$ while keeping $\alpha_2 = 0$. It can be noticed that the wave mode conversion at the joints between longitudinal and flexural waves play a significant role on the transmission coefficients of the assembly. For increasing α_1, i.e., increasing the connection angle of the beams, there is a increased attenuation from the interaction of the flexural and longitudinal band gaps. Similar results are obtained for $-\pi/2 < \alpha_1 < 0$ and for varying α_2 while keeping $\alpha_1 = 0$.

The effects of uncertainties on α_1 and α_2 at the wave mode conversion and the band gap performance are also investigated. For both considered cases, i.e. models with random variables Θ and $\mathtt{A}_1$ and $\mathtt{A}_2$, each probabilistic model considered that $\alpha_1 = \alpha_2 = 0$, with $\theta_1 = -\pi/10$ and $\theta_2 = \pi/10$, and $\mu = 0$ and $\sigma = 0.05\pi$ for parent distribution of the truncated Gaussian model. PDF curves are shown in figure 4(a). For the stochastic analysis, 1000 MC samples are used which is enough for convergence according to Eq. 10. A typical convergence curve is shown in Fig. 4(b).

Figures 5 to 8 present the mean, nominal value and MC samples of the absolute value of the transmission coefficient obtained. It can be noticed that the mean value and the nominal response are not equivalent in all of the frequency band but at the band gap regions for each longitudinal or flexural wave modes. Therefore, the deterministic analysis is not representative of the typical behaviour of the transmission coefficient outside of this regions. In fact, the results show that the nominal response gives the upper bounds of the MC samples outside the band gap regions in both cases, while it is representative of the mean response in the band gap regions. The nominal model cannot capture the wave mode conversion occurring due to the random variation of the connection angles and it cannot predict the improved attenuation features observed in these cases. Moreover, the choice of sets of random variable played a much more important role in the results than the probabilistic models for the random variables. Note that changing from uniform to a truncated Gaussian slightly affects the mean values and the tails of the distribution of the results. The model considering both connection angles and uncertainty introduced qualitative changes on the response, with frequency bands with increased attenuation performance. This is because the wave mode conversion between longitudinal and flexural waves could occur at both connections.

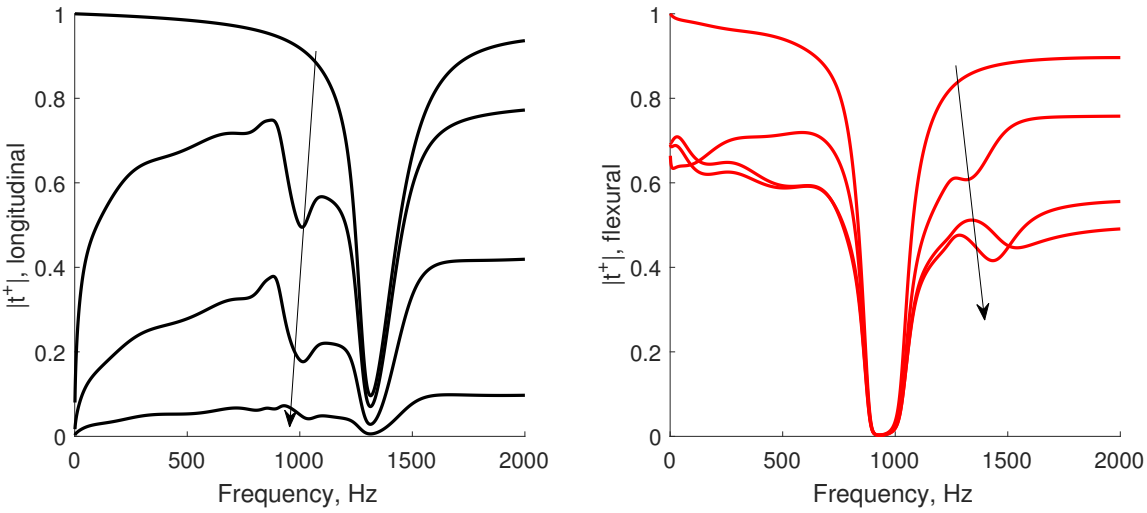

Figure 3: Absolute value of the transmission coefficient considering for increasing α_1 from 0 to $\pi/2$ and $\alpha_2 = 0$.

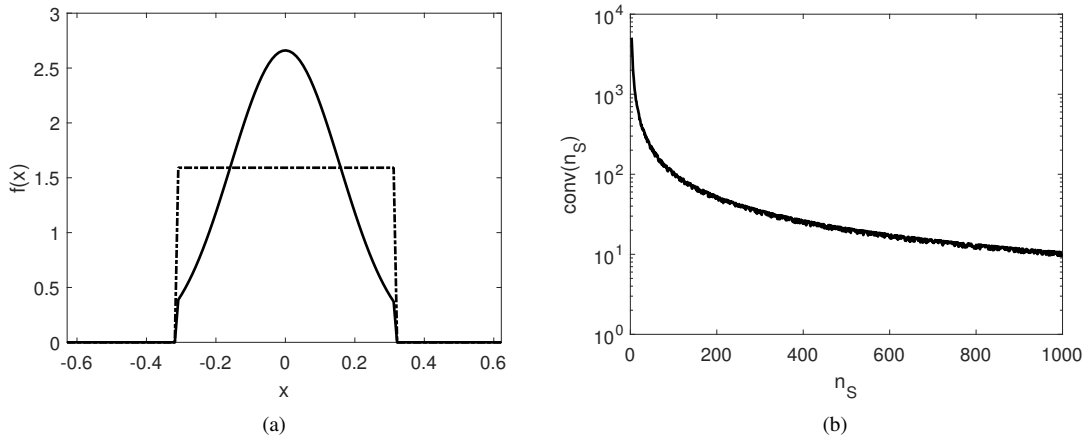

(a) (b)

Figure 4: (a) Uniform (dashed-dotted line) and truncated Gaussian (full line) PDFs used in both probabilistic models and (b) typical stochastic convergence analysis.

CONCLUDING REMARKS

The wave attenuation performance of a metamaterial beam assembly is investigated considering uncertain connections. It is assumed a large enough number of identical resonators such that and effective longitudinal and flexural wavenumbers are derived. Wave modes are assumed unchanged by the attachments and then analytical expressions can be derived. The reflection and transmission properties of the assembly are be calculated and it is shown that the angle of the assembly has a significant effect on the band gap performance.

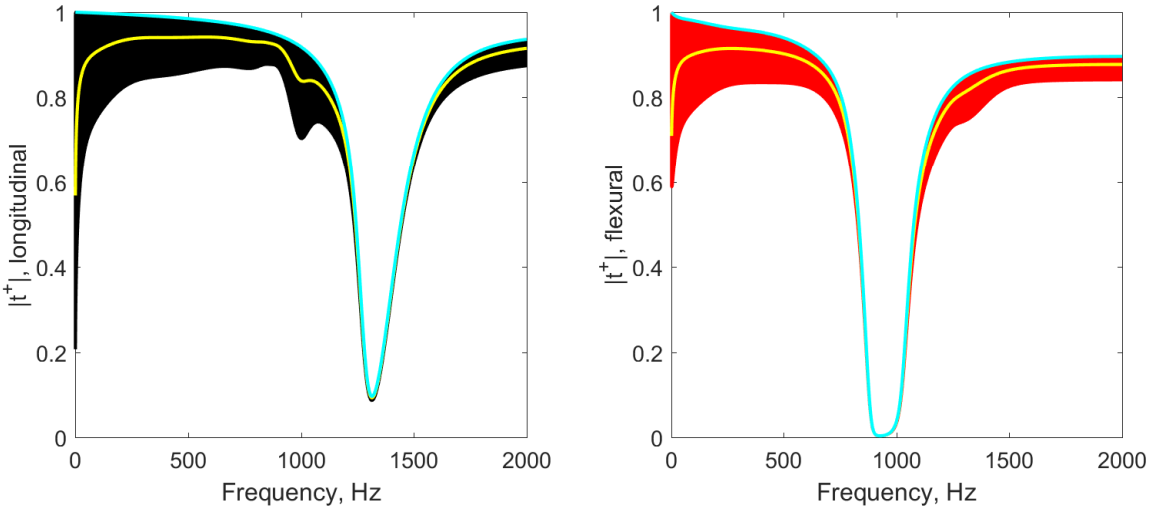

Figure 5: Mean (yellow), nominal (cyan) value and MC samples of the absolute value of the transmission coefficient considering $\alpha_1 = \alpha_2 = 0$ and Θ. Uniform PDF.

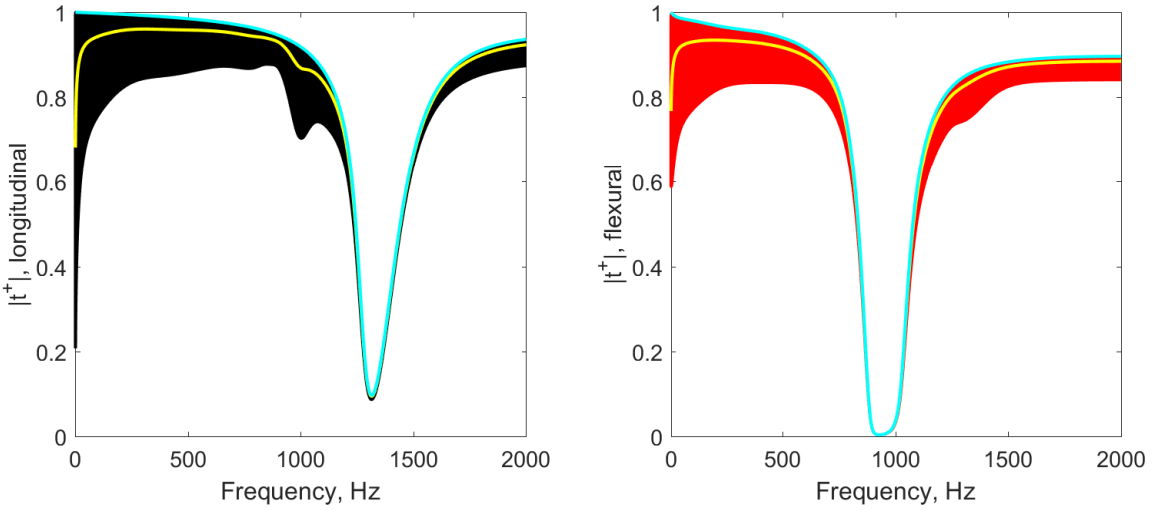

Figure 6: Mean (yellow), nominal (cyan) value and MC samples of the absolute value of the transmission coefficient considering $\alpha_1 = \alpha_2 = 0$ and Θ. Truncated Gaussian PDF.

The uncertainty analysis focus on the variability of the connection angles and ensemble statistics are investigated. Monte Carlo sampling is used as the stochastic solver. It is shown that the deterministic analysis is not representative of the typical behaviour of the transmission coefficient outside the band gap region. In this case, the nominal response gives the upper bounds of the MC samples outside the band gap regions in both cases, while it is representative of the mean response in the band gap regions.

Most importantly, it is shown that the nominal model, which does not include variability in the connections, cannot capture the wave mode conversion occurring due to the randomness of the connection angles and it cannot predict the improved attenuation features observed in these cases. Moreover, the choice of sets of random variable played a much more important role in the results than the probabilistic models for the random variables.

ACKNOWLEDGMENTS

The authors gratefully acknowledge the financial support of the Federal District Research Foundation (FAPDF) Process number 0193.001507/2017, Capes-Cofecub, project 913/18; CNPq; Faperj, and the Normandy Region.

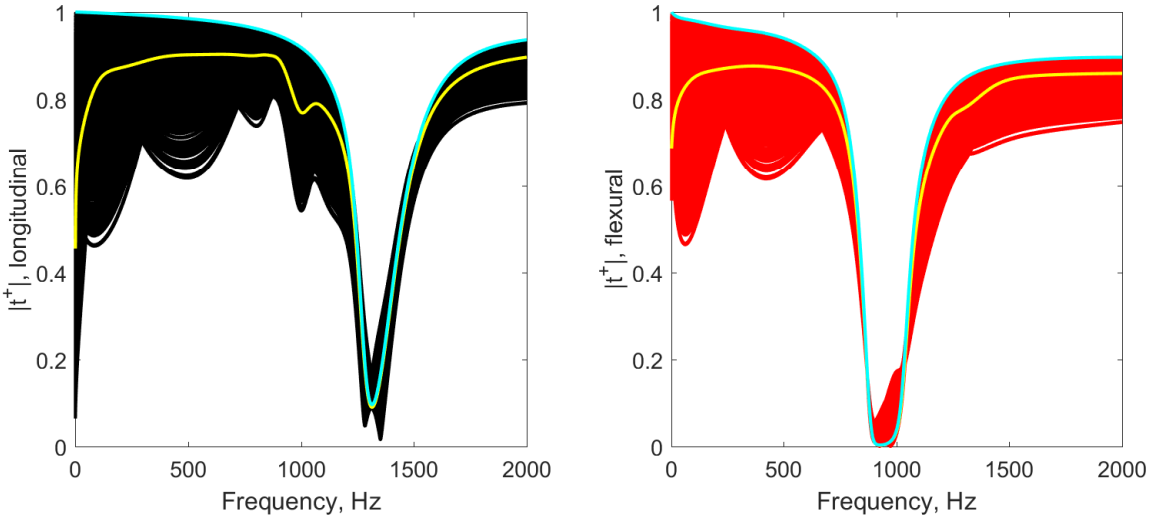

Figure 7: Mean (yellow), nominal (cyan) value and MC samples of the absolute value of the transmission coefficient considering the random variable of both connection angles, A_1 and A_2. Uniform PDF.

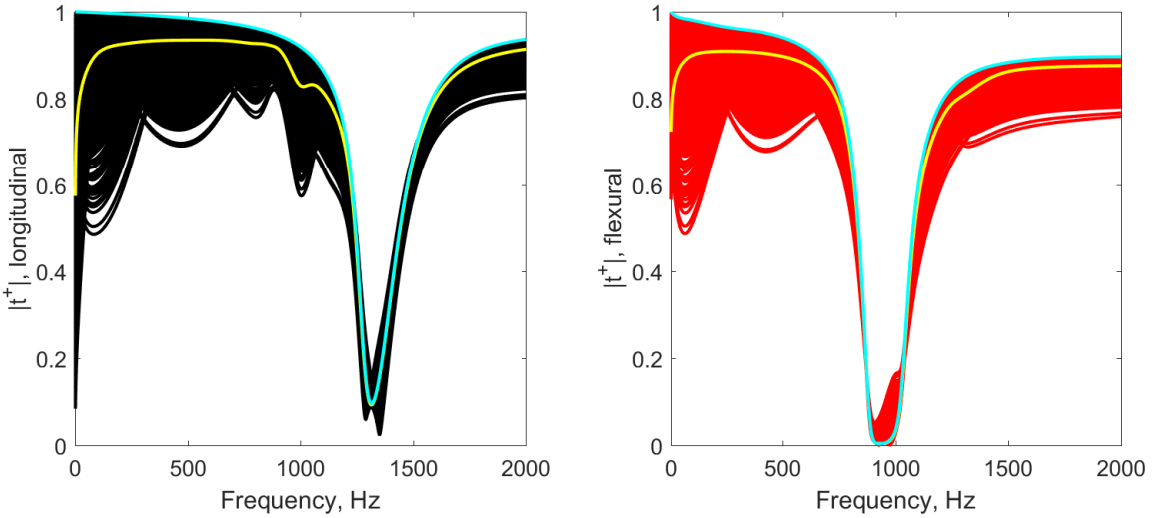

Figure 8: Mean (yellow), nominal (cyan) value and MC samples of the absolute value of the transmission coefficient considering the random variable of both connection angles, A_1 and A_2. Truncated Gaussian PDF.

REFERENCES

Arruda, J. R. F., Santos, J. M. C., Nov. 1993. Mechanical joint parameter estimation using frequency response functions and component mode synthesis. Mechanical Systems and Signal Processing 7 (6), 493–508.

Beshara, M., Keane, A. J., Jun. 1997. Vibrational energy flows in beam networks with compliant and dissipative joints. Journal of Sound and Vibration 203 (2), 321–339.

Brennan, M. J., 2006. Some Recent Developments in Adaptive Tuned Vibration Absorbers/Neutralisers. Shock and Vibration 13 (4-5), 531–543.

Den Hartog, J., 1985. Mechanical Vibrations. Civil, Mechanical and Other Engineering Series. Dover Publications.

Dohnal, F., Mace, B. R., Ferguson, N. S., 2009. Joint Uncertainty Propagation in Linear Structural Dynamics Using Stochastic Reduced Basis Methods. AIAA Journal 47 (4), 961–969.

Fabro, A. T., Beli, D., Arruda, J. R. F., Ferguson, N. S., Mace, B., 2016. Uncertainty analysis of band gaps for beams with periodically distributed resonators produced by additive manufacturing. In: ISMA 2016 Conference on Noise and Vibration Engineering. Leuve, Belgium, p. 12.

Fabro, A. T., Ferguson, N. S., Jain, T., Halkyard, R., Mace, B. R., 2015. Wave propagation in one-dimensional waveguides with slowly varying random spatially correlated variability. Journal of Sound and Vibration 343, 20–48.

Fabro, A. T., Mencik, J.-M., 2018. On the non-parametric modelling of uncertain elastic joints in periodic structures. In: Proceedings of the International Conference on Noise and Vibration Engineering (ISMA2018/USD2018). Leuven,

Belgium.
Fan, Y., Collet, M., Ichchou, M., Li, L., Bareille, O., Dimitrijevic, Z., 2016. A wave-based design of semi-active piezoelectric composites for broadband vibration control. Smart Materials and Structures 25 (5), 055032.
Gao, Y., Brennan, M. J., Sui, F., Jun. 2011. Control of flexural waves on a beam using distributed vibration neutralisers. Journal of Sound and Vibration 330 (12), 2758–2771.
Harland, N. R., Mace, B. R., Jones, R. W., 2001. Wave propagation, reflection and transmission in tunable fluid-filled beams. Journal of Sound and Vibration 241, 735–754, 5.
Huang, H. H., Sun, C. T., 2009. Wave attenuation mechanism in an acoustic metamaterial with negative effective mass density. New Journal of Physics 11 (1), 013003.
Hussein, M. I., Leamy, M. J., Ruzzene, M., 2014. Dynamics of phononic materials and structures: Historical origins, recent progress, and future outlook. Applied Mechanics Reviews 66 (4), 040802–040802–38.
Ibrahim, R. A., Pettit, C. L., Jan. 2005. Uncertainties and dynamic problems of bolted joints and other fasteners. Journal of Sound and Vibration 279 (3), 857–936.
Liu, Z., Zhang, X., Mao, Y., Zhu, Y. Y., Yang, Z., Chan, C. T., Sheng, P., 2000. Locally resonant sonic materials. Science 289 (5485), 1734–1736.
Mace, B. R., Jun. 2014. Discussion of Dynamics of Phononic Materials and Structures: Historical Origins, Recent Progress and Future Outlook (Hussein, M. I., Leamy, M. J., and Ruzzene, M., 2014, ASME Appl. Mech. Rev., 66(4), p. 040802). Applied Mechanics Reviews 66 (4), 045502–045502.
Muggleton, J. M., Waters, T. P., Mace, B. R., Zhang, B., Oct. 2007. Approaches to estimating the reflection and transmission coefficients of discontinuities in waveguides from measured data. Journal of Sound and Vibration 307 (1), 280–294.
Rubinstein, R., Kroese, D., 2007. Simulation and the Monte Carlo method, second edition Edition. Wiley Series in Probability and Statistics. John Wiley & Sons, Inc., Hoboken, NJ, USA.
Sugino, C., Xia, Y., Leadenham, S., Ruzzene, M., Erturk, A., Oct. 2017. A general theory for bandgap estimation in locally resonant metastructures. Journal of Sound and Vibration 406 (Supplement C), 104–123.
Zhang, B., Waters, T. P., Mace, B. R., Apr. 2010. Identifying joints from measured reflection coefficients in beam-like structures with application to a pipe support. Mechanical Systems and Signal Processing 24 (3), 784–795.

RESPONSIBILITY NOTICE

The authors are the only responsible for the printed material included in this paper.

APPENDIX

Dispersion equation with attached resonators

In this section, the dispersion equation of a one-dimensional metastructure is derived. It is considered a continuous system with S attached resonators, then Eq. 4 can be derived as the governing equation (Sugino et al., 2017). Assuming time harmonic motion, i.e. $w(x,t) = W(x)e^{i\omega t}$ and $u_p(x,t) = U_p e^{i\omega t}$ for the p^{th} resonator, then

$$L(x)W(x) - \omega^2 \mu W(x) - \sum_{p=1}^{S} k_p U_p \delta(x - x_p) = P(x) \quad \text{and} \quad -\omega^2 m_p U_p - \omega^2 m_p W(x_p) + k_p U_p = 0. \tag{11}$$

From the second equation, it is possible to find $U_p = \omega^2/(\omega_p^2 - \omega^2)W(x_p)$, where $\omega_p^2 = k_p/m_p$. Substituting back in the first equation, then

$$L(x)W(x) - \omega^2 \mu W(x) - \sum_{p=1}^{S} k_p \frac{\omega_p^2}{\omega_p^2 - \omega^2} W(x_p)\delta(x - x_p) = P(x). \tag{12}$$

Assuming a constant mass ratio, i.e., $m_p = \varepsilon \mu \Delta l$, where Δl is the distance between resonators, and identical resonators such that $\omega_p = \omega_r$, $p = 1, 2, ...$, then

$$L(x)W(x) - \omega^2 \mu W(x) - \varepsilon \mu \omega^2 \frac{\omega_r^2}{\omega_r^2 - \omega^2} \sum_{p=1}^{S} W(x_p)\delta(x - x_p)\Delta l = P(x). \tag{13}$$

Assuming a large enough number of resonators, the following approximation can be made

$$\lim_{S\to\infty} \sum_{p=1}^{S} W(x_p)\delta(x - x_p)\Delta l \approx \int_{-\infty}^{\infty} W(\xi)\delta(\xi - x)d\xi = W(x), \tag{14}$$

which yields

$$L(x)W(x) - \omega^2 \mu \left(1 + \varepsilon \frac{1}{1-\Omega_r^2}\right) W(x) = P(x), \tag{15}$$

where $\Omega_r = \omega_r/\omega$. Assuming space harmonic motion $W(x) = \tilde{W}e^{-ikx}$, the dispersion equation for beam with attached resonators is given by Eq. 5.

Scattering matrix

In this section, reflection and transmission matrices are derived for the metamaterial beam assembly shown in Fig. 1. Assuming two connected waveguides i and j, Eq. 3 can be used to describe the displacement $\mathbf{q}_i$ and $\mathbf{q}_j$ and internal forces $\mathbf{f}_i$ and $\mathbf{f}_j$, respectively. Continuity and equilibrium conditions can be defined by the matrix relation $\mathbf{C}_i\mathbf{q}_i = \mathbf{C}_j\mathbf{q}_j$ and $\mathbf{E}_i\mathbf{f}_i = \mathbf{E}_j\mathbf{q}_j$ (Harland et al., 2001; Fabro et al., 2015). A scattering matrix $\mathbf{G}$ can be defined at each waveguide connection `a` and `b` by

$$\begin{bmatrix} \mathbf{b}_2^+ \\ \mathbf{b}_2^- \end{bmatrix} = \mathbf{G}_\mathtt{b} \begin{bmatrix} \mathbf{b}_1^+ \\ \mathbf{b}_1^- \end{bmatrix}, \quad \text{and} \quad \begin{bmatrix} \mathbf{a}_2^+ \\ \mathbf{a}_2^- \end{bmatrix} = \mathbf{G}_\mathtt{a} \begin{bmatrix} \mathbf{a}_1^+ \\ \mathbf{a}_1^- \end{bmatrix}. \tag{16}$$

Applying continuity and equilibrium conditions and assuming the matrix inversion exists, thus

$$\mathbf{G}_\mathtt{b} = \begin{bmatrix} \mathbf{C}_{2\mathtt{b}}\Phi^+_{q2\mathtt{b}} & \mathbf{C}_{2\mathtt{b}}\Phi^-_{q2\mathtt{b}} \\ \mathbf{E}_{2\mathtt{b}}\Phi^+_{f2\mathtt{b}} & \mathbf{E}_{2\mathtt{b}}\Phi^-_{f2\mathtt{b}} \end{bmatrix}^{-1} \begin{bmatrix} \mathbf{C}_{1\mathtt{b}}\Phi^+_{q1\mathtt{b}} & \mathbf{C}_{1\mathtt{b}}\Phi^-_{q1\mathtt{b}} \\ \mathbf{E}_{1\mathtt{b}}\Phi^+_{f1\mathtt{b}} & \mathbf{E}_{1\mathtt{b}}\Phi^-_{f1\mathtt{b}} \end{bmatrix}, \tag{17}$$

and

$$\mathbf{G}_\mathtt{a} = \begin{bmatrix} \mathbf{C}_{1\mathtt{a}}\Phi^+_{q1\mathtt{a}} & \mathbf{C}_{1\mathtt{a}}\Phi^-_{q1\mathtt{a}} \\ \mathbf{E}_{1\mathtt{a}}\Phi^+_{f1\mathtt{a}} & \mathbf{E}_{1\mathtt{a}}\Phi^-_{f1\mathtt{a}} \end{bmatrix}^{-1} \begin{bmatrix} \mathbf{C}_{2\mathtt{a}}\Phi^+_{q2\mathtt{a}} & \mathbf{C}_{2\mathtt{a}}\Phi^-_{q2\mathtt{a}} \\ \mathbf{E}_{2\mathtt{a}}\Phi^+_{f2\mathtt{a}} & \mathbf{E}_{2\mathtt{a}}\Phi^-_{f2\mathtt{a}} \end{bmatrix}, \tag{18}$$

where the subscripts $\mathtt{1a}, \mathtt{1b}, \mathtt{2a}$ and $\mathtt{2b}$ stand for the waves at the left and right side of each junction and connection `a` and `b`, respectively, as shown in Fig 1. For a beam undergoing longitudinal and bending vibration, then

$$\Phi_q^+ = \begin{bmatrix} 1 & 0 & 0 \\ 0 & 1 & 1 \\ 0 & -ik_b & -k_b \end{bmatrix}, \qquad \Phi_q^- = \begin{bmatrix} 1 & 0 & 0 \\ 0 & 1 & 1 \\ 0 & ik_b & k_b \end{bmatrix}, \tag{19}$$

$$\Phi_f^+ = \begin{bmatrix} -iEAk_l & 0 & 0 \\ 0 & -iEIk_b^3 & EIk_b^3 \\ 0 & -EIk_b^2 & EIk_b^2 \end{bmatrix}, \qquad \Phi_f^- = \begin{bmatrix} iEAk_l & 0 & 0 \\ 0 & iEIk_b^3 & -EIk_b^3 \\ 0 & -EIk_b^2 & EIk_b^2 \end{bmatrix}. \tag{20}$$

In the metamaterial beams, assuming that the attached resonators do not change the wave types, the longitudinal k_l and bending k_b wavenumber are simply replaced by the effective wavenumbers k_{lr} and k_{br}. Moreover, a scattering matrix of the metamaterial assembly can be defined as

$$\begin{bmatrix} \mathbf{a}_2^+ \\ \mathbf{a}_2^- \end{bmatrix} = \mathbf{G} \begin{bmatrix} \mathbf{b}_1^+ \\ \mathbf{b}_1^- \end{bmatrix}, \quad \mathbf{G} = \mathbf{G}_a \Lambda \mathbf{G}_b, \tag{21}$$

where $\Lambda = \mathtt{diag}\left[e^{-ik_{rl}L}, e^{-ik_{rb}L}, e^{-k_{rl}L}, e^{ik_{rl}L}, e^{ik_{rb}L}, e^{k_{rl}L}\right]$, L is the metamaterial beam length, k_{rl} and k_{rb} are longitudinal and bending metamaterial effective wavenumbers, from Eq. 6, and `diag` stands for diagonal matrix. It is also possible to write the scattering in terms of incoming and outgoing waves, as given by Eq. 7, using reflection and transmission matrices. It can be shown that (Harland et al., 2001; Fabro et al., 2015)

$$\mathbf{r}^+ = \mathbf{G}_{12}\mathbf{G}_{22}^{-1}, \mathbf{t}^+ = \mathbf{G}_{11} - \mathbf{G}_{12}\mathbf{G}_{22}^{-1}\mathbf{G}_{21}, \mathbf{t}^- = \mathbf{G}_{22}^{-1}, \mathbf{r}^- = -\mathbf{G}_{22}^{-1}\mathbf{G}_{21} \tag{22}$$

The continuity and equilibrium matrices are given by

$$\mathbf{C}_{1\mathtt{b},2\mathtt{a}} = \mathbf{E}_{1\mathtt{b},2\mathtt{a}} = \begin{bmatrix} 1 & 0 & 0 \\ 0 & 1 & 0 \\ 0 & 0 & 1 \end{bmatrix}, \mathbf{C}_{2\mathtt{b},1\mathtt{a}} = \mathbf{E}_{2\mathtt{b},1\mathtt{a}} = \begin{bmatrix} \cos\alpha_{1,2} & \sin\alpha_{1,2} & 0 \\ -\sin\alpha_{1,2} & \cos\alpha_{1,2} & 0 \\ 0 & 0 & 1 \end{bmatrix}, \tag{23}$$